AIP | The Journal of Chemical Physics

Chain architecture and micellization: A mean-field coarse-grained model for poly(ethylene oxide) alkyl ether surfactants

Fabián A. García Daza, Alexander J. Colville, and Allan D. Mackie

Citation: The Journal of Chemical Physics **142**, 114902 (2015); doi: 10.1063/1.4913960
View online: http://dx.doi.org/10.1063/1.4913960
View Table of Contents: http://scitation.aip.org/content/aip/journal/jcp/142/11?ver=pdfcov
Published by the AIP Publishing

Chain architecture and micellization: A mean-field coarse-grained model for poly(ethylene oxide) alkyl ether surfactants

Fabián A. García Daza,[1] Alexander J. Colville,[2] and Allan D. Mackie[1,a)]
[1]*Department d'Enginyeria Química, ETSEQ, Universitat Rovira i Virgili, Avinguda dels Països Catalans 26, 43007 Tarragona, Spain*
[2]*Department of Chemical Engineering, Northeastern University, 360 Huntington Avenue, Boston, Massachusetts 02115-5000, USA*

(Received 24 December 2014; accepted 12 February 2015; published online 16 March 2015)

Microscopic modeling of surfactant systems is expected to be an important tool to describe, understand, and take full advantage of the micellization process for different molecular architectures. Here, we implement a single chain mean field theory to study the relevant equilibrium properties such as the critical micelle concentration (CMC) and aggregation number for three sets of surfactants with different geometries maintaining constant the number of hydrophobic and hydrophilic monomers. The results demonstrate the direct effect of the block organization for the surfactants under study by means of an analysis of the excess energy and entropy which can be accurately determined from the mean-field scheme. Our analysis reveals that the CMC values are sensitive to branching in the hydrophilic head part of the surfactant and can be observed in the entropy-enthalpy balance, while aggregation numbers are also affected by splitting the hydrophobic tail of the surfactant and are manifested by slight changes in the packing entropy. © *2015 AIP Publishing LLC.* [http://dx.doi.org/10.1063/1.4913960]

I. INTRODUCTION

Copolymer surfactants are widely used in industry for a variety of applications where their ability to self-assemble into micelles is key to their performance. For example, these micellar systems are of great utility for the drug delivery of pharmaceuticals, gene therapy, nanomaterial synthesis, food processing, and oil spill recovery.[1] As a result of the many applications of copolymer surfactants, much research has been conducted on the properties and molecular characteristics of them. Since the surfactants amphiphilic properties drive the self-assembly into micelles, the molecular structure of the surfactants is an essential part of the process. It is thus of great significance to fully understand and predict the effects of surfactant architecture on micelle thermodynamic properties as a step towards the design of tailor made surfactants for specific applications.

Many previous experimental works and reviews have looked at the utility of polymer architecture in drug delivery[2–6] and other applications. For example, Nakamura *et al.*[7] found star polymers to enhance therapeutic efficacy and antitumor activity in comparison to linear polymers when conjugated to drugs. These works highlight the promising potential for tailoring surfactant structure for unique and desirable characteristics. Numerous previous experimental works have sought to understand the thermodynamic properties behind the self-assembly of these complex surfactant shapes using techniques such as surface tension,[8] static and dynamic light scattering,[9] elution gel-permeation chromatography, dye solubilization,[10] electrical conductivity measurement, steady-state fluorescence measurement,[11,12] and microcalorimetry[13] to study critical micelle concentrations (CMCs) and aggregations numbers. Such experimental works have covered a variety of architectures including diblock, triblock, ring, gemini, bolaform, and branched among others.[14] However, time, cost, and accuracy constraints have spurred researchers in this field to pursue simulations in their study of copolymer characterization.[15] The experimental results have shown that there is a very wide parameter space to explore the effect of architecture on micelle formation.[16] The large variable space can be covered more cost effectively with simulations that are capable of providing detail on a more microscopic level than current experimental techniques. However, little simulation work has been done so far to investigate the effect of surfactant structure on micellar properties systematically.[17]

A few works have previously simulated the properties of copolymer micelles based on the effects of surfactant architecture using Molecular Dynamics (MD) simulations.[18,19] La Rosa *et al.*[18] investigated monolayers of surfactants with MD successfully. However, MD has limitations in the intensive computational power that the technique requires and the time scales necessary to reach equilibrium. While atomistic molecular simulations allow for greater accuracy and detail of the particles, mesoscale simulations allow for the study of larger surfactants over longer periods of time using coarse-graining. As a direct result, several groups have used Dissipative Particle Dynamics (DPD) to investigate the effects of block architecture.[20] For similar reasons, a lot of work utilizes Monte Carlo (MC) simulations in this area of research. Between DPD and MC, the available published work has looked at the effect of surfactant architecture in monolayers,[21] bilayer membranes,[22] and micelles.[23,24] These simulations have shown

a)Electronic mail: allan.mackie@urv.cat

success in investigating thermodynamic and micellar properties such as CMC and aggregation number for a great variety of surfactant architectures, in particular, Panagiotopoulos *et al.*[25] studied the micellization, CMC, and phase separation conditions for a series of diblocks, TH, and triblocks, THT and HTH, surfactants in a lattice grand-canonical MC. The abbreviation H is used for the head or hydrophilic group and T for the tail or hydrophobic group. In a similar fashion, Kim and Jo[26] studied the aggregation numbers and CMC for THT and HTH block copolymers, predicting higher values of both quantities for the HTH system at a fixed temperature, and a quantitative description of the aggregation process was analyzed in terms of the enthalpic and entropic contributions derived from the simulations.[26,27] Rekvig *et al.*[28] combined DPD and MC to test the impact of chain geometry for linear and branched surfactants on their efficiency at the oil-water interface yielding an advantage for branched molecules in terms of adsorbance and free monomer concentration in the bulk. Jackson *et al.*,[29] by means of a two-dimensional MC, studied the effect of asymmetry for a fixed number of hydrophobic/hydrophilic units for linear surfactants exhibiting a strong dependence on the CMC with respect to the number of spacers in the gemini-like case in comparison to the asymmetry. Also, mean-field techniques like the Self-Consistent Field (SCF) theory have been employed to describe the micellization process for series of surfactants. In this theory, polymers in solution are assumed to be ideal chains surrounded by interacting fields and it is possible to study equilibrium and geometrical properties of copolymers systems. Zhou and Shi[30] studied the most stable shape from one-dimensional simulations for linear diblock surfactants with different lengths. Hurter *et al.*[31] compared the partition coefficients in the case of triblock and Tetronic Pluronics when solubilized with different compounds. Symmetric surfactants have also been widely studied predicting phase behavior,[32,33] CMC, critical micelle temperature, and cloud point temperature.[34,35] In addition, symmetric and asymmetric THT and HTH triblocks have been studied by Monzen *et al.*[36] resulting in a more favorable formation of spherical micelles for the symmetric HTH case with respect to the THT system while the opposite case is true when the end blocks are highly asymmetric.

To our knowledge, there are only a very limited amount of simulation works, e.g., employing DPD and MC, that have quantitatively compared results with experimental findings. More research remains to be completed in order to fully understand the connection between DPD atomistic length-scale simulations and macroscopic experimental results. In addition, the discrete lattice model used in the MC and SCF simulations also causes difficulties in comparing directly to experimental results. Because of these limitations of previous works, this work utilizes the Single Chain Mean Field (SCMF) theory[37] that has been successfully used in previous studies of surfactant systems to predict and compare quantitatively with available experimental data.[38] The SCMF is a mean-field technique that is similar in spirit to SCF, nevertheless, the main difference comes from the connectivity related to the chains representing the surfactants; in the SCF scheme, the chains are ideal which means that they are Markovian in nature implying the possibility of the presence of overlapping configurations. In contrast, the SCMF considers non-Markovian chains leading to non-overlapping conformations, which allows for the explicit consideration of the excluded-volume interactions that are not considered in SCF.[39] This is essential in the present work where different chain architectures are compared and can be expected to have a direct impact on the free energy of the system. In particular, this paper seeks to further the study of the effects of surfactant architecture with a comparison between simulation values for CMCs and aggregation numbers across a more comprehensive set of surfactant structures: diblock (linear), branched, gemini, and triblock. The study also compares directly to experimental data when available.

II. SIMULATION AND MODEL DETAILS

A. Single chain mean field theory

The SCMF theory[37] is a free energy model that is based on the individual contributions of a single chain that belongs to the set of permitted conformations $\{\alpha\}$ representing the surfactant by means of its interaction with surrounding fields of solvent and surfactants. This is provided in the assignation of an individual probability $P[\alpha]$ for every conformation which leads to the calculation of average properties in equilibrium over these probabilities, particularly, the entropic and energetic effects due to the surfactant molecular structure. The starting point in the theory is the consideration of the explicit Helmholtz free energy F_N for an aggregate of size N,

$$F_N = \langle U_N \rangle - T\langle S_N \rangle, \tag{1}$$

where the first and the second terms refer to the energetic and the entropic contributions, respectively, and are defined by

$$\langle U_N \rangle = N \int d\alpha P[\alpha] U(\alpha, c_s(\vec{r})), \tag{2}$$

with $U(\alpha, c_s(\vec{r})) = U_{intra}(\alpha) + U_{inter}(\alpha, c_s(\vec{r}))$ as the total intramolecular and intermolecular energies for the corresponding conformation α depending on the solvent concentration $c_s(\vec{r})$. The exact form depends on the coarse-grained model chosen to represent the surfactant molecules and solvent as will be shown below. On the other hand, the entropy of surfactants and solvent is expressed as

$$\langle S_N \rangle = -kN \int d\alpha P[\alpha] \ln P[\alpha] - k \int d\vec{r} c_s(\vec{r}) \ln \phi_s(\vec{r}),$$

with k as the Boltzmann constant and $\phi_s(\vec{r}) = v_s c_s(\vec{r})$ the solvent volume fraction where v_s is the solvent bead volume. To determine the equilibrium state, it is necessary to minimize the free energy in Eq. (1) together with the volume-filling constraint, $\phi_s(\vec{r}) + N\langle \varphi_{exc}(\vec{r}) \rangle = 1$ by means of a Lagrange multiplier $\pi(\vec{r})$, where the second term is the volume fraction of the aggregate occupying the point $\vec{r}$. The physical meaning of the constraint resides in the condition that all regions of space are occupied by either surfactant or solvent molecules deriving from the steric hard-core repulsions for surfactant molecules. As can be observed from the expressions for $\langle U_N \rangle$ and $\langle S_N \rangle$, variations in the free energy depend on changes of the single-chain probabilities $P[\alpha]$ and the solvent concentration $c_s(\vec{r})$ leading to complete the minimization procedure from

the evaluation of the functional derivatives $\delta F_N/\delta P[\alpha] = 0$ and $\delta F_N/\delta c_s(\vec{r}) = 0$. As expected, this provides an expression for $P[\alpha] = e^{-H_N(\alpha)/kT}/Q$ which depends on $c_s(\vec{r})$ through the effective SCMF Hamiltonian $H_N(\alpha)$ and therefore the partition function Q ensuring $1 = \int d\alpha P[\alpha]$. Generally, the explicit form of $U(\alpha, c_s(\vec{r}))$ depends on the surfactant model and the intra and intermolecular interactions taken into account, while the expression for $P[\alpha]$ is influenced by the approximations considered in the minimization process. In this work, we consider a series of surfactants with different arrangements of the hydrophilic and hydrophobic units, where in order to describe the moieties involved, we implement the model developed by Gezae Daful *et al.*[38] for nonionic poly(ethylene oxide) alkyl ethers, where hydrophobic CH_2, hydrophilic CH_2CH_2O, and solvent groups are represented by beads of diameter σ. The distance between the centers of two consecutive beads belonging to the same surfactant is taken to be 1.42σ. The intermolecular interactions considered in the model are included via square well potentials with the corresponding volume $4\pi(r_{int}^3 - \sigma^3)/3$ from the center of each bead with $r_{int} = 1.61\sigma$. This potential has a depth ε, given in kT units, that depends on the interactions taken into account which in this case are those between hydrophobic, C, and hydrophilic, EO, and the solvent medium, S ($\varepsilon_{C,EO}$, $\varepsilon_{C,S}$ and $\varepsilon_{EO,S}$). From these considerations, the interaction energy for configuration α in this coarse-grained is taken to be

$$U(\alpha, c_s(\vec{r})) \approx U_{intra}(\alpha) + \frac{N-1}{2}\varepsilon_{C,EO}\int d\vec{r}d\beta P[\beta]\left(\Phi_C(\alpha,\vec{r})c_{EO}(\beta,\vec{r}) + \Phi_{EO}(\alpha,\vec{r})c_C(\beta,\vec{r})\right) + \int d\vec{r}\left(\varepsilon_{C,S}\Phi_C(\alpha,\vec{r}) + \varepsilon_{EO,S}\Phi_{EO}(\alpha,\vec{r})\right)c_s(\vec{r}), \tag{3}$$

the first term is calculated as the interaction energy $\varepsilon_{C,EO}$ times the number of non-consecutive intramolecular EO–C contacts for conformation α whose distance between centers lie in the range $[\sigma, 1.61\sigma]$, the second term indicates the interaction of conformation α through the available interaction volume $d\vec{r}\Phi(\alpha,\vec{r})$ at $\vec{r}$ with concentration fields $c(\beta,\vec{r})$ of conformation β for species EO and C, while the third term is the corresponding interaction of conformation α with the solvent medium (water). Once the interaction terms are known and the free energy minimization procedure is completed, the SCMF probabilities that minimize the free energy are found be

$$P[\alpha] = \frac{1}{Q}\exp\left[-\frac{1}{kT}\left(U_{intra}(\alpha) + (N-1)\varepsilon_{C,EO} \times \int d\vec{r}\left(\Phi_C(\alpha,\vec{r})\langle c_{EO}(\vec{r})\rangle + \Phi_{EO}(\alpha,\vec{r})\langle c_C(\vec{r})\rangle\right) + \int d\vec{r}\left(\varepsilon_{C,S}\Phi_C(\alpha,\vec{r}) + \varepsilon_{EO,S}\Phi_{EO}(\alpha,\vec{r})\right)c_s(\vec{r}) - \frac{kT}{v_s}\int d\vec{r}\phi_{ex}(\alpha,\vec{r})\ln\phi_s(\vec{r})\right)\right], \tag{4}$$

where the term in the exponential is referred to as the SCMF Hamiltonian $H_N(\alpha)$ for conformation α. We have used the averaged value for the concentration fields of the surfactant $\langle c(\vec{r})\rangle = \int d\alpha P[\alpha]c(\alpha,\vec{r})$ that along with Eq. (4) and the incompressibility condition forms a set of non-linear equations which can be solved iteratively giving as a result the values of $P[\alpha]$, $c_s(\vec{r})$ and hence $\langle c_{EO}(\vec{r})\rangle$ and $\langle c_C(\vec{r})\rangle$ for an aggregate of size N which ensures the minimum value of the free energy of the system given in Eq. (1).

B. Equilibrium properties

The connection between the microscopic nature and the macroscopic observables, particularly, the CMCs and concentration of aggregates in equilibrium is provided by the multiple equilibrium model[40]

$$\frac{X_N}{N} = X_1^N e^{-N(\mu_N^0 - \mu_1^0)/kT}, \tag{5}$$

where X_N and X_1 are the concentrations of surfactants in aggregates of size N and in the bulk, respectively, with their corresponding standard chemical potentials μ_N^0 and μ_1^0, which, in turn, can be obtained from the SCMF simulations[41]

$$\frac{\mu_N^0 - \mu_1^0}{kT} = -\log\left(\frac{V}{N}\frac{\sum_\alpha e^{-H_N(\alpha)/kT}/W(\alpha)}{\sum_\alpha e^{-H_1(\alpha)/kT}/W(\alpha)}\right), \tag{6}$$

with V as the volume of the simulation box, $W(\alpha)$, the corresponding correction to the bias generated in the generation of non-overlapping conformations according to the Rosenbluth and Rosenbluth method,[42] and $H_N(\alpha)$ and $H_1(\alpha)$, the SCMF Hamiltonians for surfactants in aggregates of size N and in the bulk solution respectively, which can be determined from Eq. (4)

$$H_N(\alpha) \approx U_{intra}(\alpha) + (N-1)\varepsilon_{C,EO} \times \int d\vec{r}\left(\Phi_C(\alpha,\vec{r})\langle c_{EO}(\vec{r})\rangle + \Phi_{EO}(\alpha,\vec{r})\langle c_C(\vec{r})\rangle\right) + \int d\vec{r}\left(\varepsilon_{C,S}\Phi_C(\alpha,\vec{r}) + \varepsilon_{EO,S}\Phi_{EO}(\alpha,\vec{r})\right)c_s(\vec{r}) - \frac{kT}{v_s}\int d\vec{r}\phi_{ex}(\alpha,\vec{r})\ln\phi_s(\vec{r}). \tag{7}$$

In order to compare the effect of chain architecture on the energetic and entropic quantities in equilibrium, we can use the relation between the standard chemical potentials and the excess enthalpy and entropy per molecule[26]

$$\frac{\mu_N^0 - \mu_1^0}{kT} = \frac{\Delta U^0}{kT} - \frac{\Delta S^0}{k}, \tag{8}$$

TABLE I. Surfactant chain architectures considered in this work.

Type	Chemical structure	Abbreviation
Diblock (linear)	$H(CH_2)_n(OCH_2CH_2)_mOH$	C_nE_m
Branched	$[H(CH_2)_{n/2-1}]_2CHCH_2(OCH_2CH_2)_mOH$	IC_nE_m
Gemini	$[H(CH_2)_{n/2-2}CHCH_2(OCH_2CH_2)_{m/2}OH]_2$	Gem_nE_m
Triblock	$HO(CH_2CH_2O)_{m/2}(CH_2)_n(OCH_2CH_2)_{m/2}OH$	$E_{m/2}C_nE_{m/2}$
Triblock	$H(CH_2)_{n/2}(OCH_2CH_2)_m(CH_2)_{n/2}H$	$C_{n/2}E_mC_{n/2}$

where the term on the left is given by SCMF calculations from Eq. (6), while the excess enthalpy representing the energetic favorability in the aggregation process, $\Delta U^0 = \langle U_N \rangle / N - \langle U_1 \rangle$, for surfactants in aggregates and in the bulk solution can be obtained directly from the evaluation of Eq. (2). Once the standard chemical potential and the excess enthalpic contributions are known, using Eq. (8) it is possible to calculate the entropy of packing surfactants with a very-well defined architecture in equilibrium aggregates, $\Delta S^0 = \langle S_N \rangle / N - \langle S_1 \rangle$. This quantity is related to the equilibrium size of the micelles depending on the surfactant geometry[26,43] as has previously been demonstrated for linear diblock and triblock copolymers. The use of Eq. (8) to calculate ΔS^0 is required to avoid translational entropic contributions contained in the SCMF formalism and is based on the standard chemical potential[41] and the energetic terms which are independent of the translational degrees of freedom. The determination of the enthalpic and entropic excess contributions enables us to directly analyze the effect of chain architecture on the relevant equilibrium properties such as the equilibrium aggregation number N_{agg} and CMC. In this work, the CMC is defined as the exponential of the minimum value of the standard chemical difference, namely, $CMC \approx \exp((\mu^0_{N_{agg}} - \mu^0_1)/kT)$. We have chosen four types of surfactants with different hydrophobic and hydrophilic block architectures as given in Table I. Examples of the different types of surfactants with various chain lengths can be observed in Figure 1 where typical configurations of surfactants in aggregates are shown. Note that the conformations are non-overlapping and flexible and were generated based on the Rosenbluth and Rosenbluth algorithm.[42]

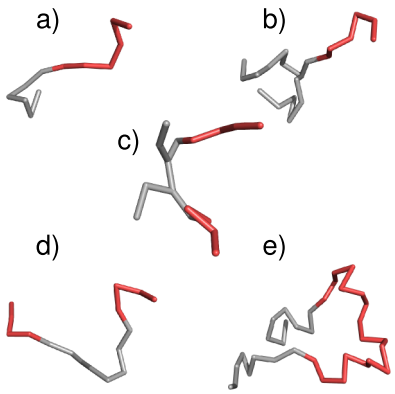

FIG. 1. Chain architectures studied using the SCMF scheme: (a) linear, (b) branched, (c) gemini and triblock with (d) hydrophobic and (e) hydrophilic central chains. In all cases, red and gray sticks refer to hydrophilic and hydrophobic units, respectively. The beads representing the moieties are omitted to represent the surfactants in a clear manner.

A series of simulations using a parallel OpenMP environment were performed for a set of 10 million conformations $\{\alpha\}$ for each surfactant system in simulation boxes with volumes between $(25\sigma)^3$ and $(60\sigma)^3$ depending on the total length of the surfactant under study. A one-dimensional spherical geometry has been assumed to discretize all the fields, this choice is due to our interest in the properties related to the initial appearance of micelles close to the CMC,[44,45] neglecting then the possibility of shape transitions which is beyond of the scope of this work. Both, 24-core and 32-core AMD workstations with RAM memories of 32 Gb and 128 Gb respectively, were used. After solving the SCMF equations, we obtained the standard chemical potential difference, $(\mu^0_{N_{agg}} - \mu^0_1)/kT$, the concentration profiles for each aggregate and solvent, $\langle c_C(\vec{r}) \rangle$, $\langle c_{EO}(\vec{r}) \rangle$, and $c_s(\vec{r})$, together with the probabilities distribution, $\{P[\alpha]\}$, the excess enthalpy contributions, ΔU^0, and from here the excess or packing entropy per surfactant, ΔS^0.

III. RESULTS AND DISCUSSION

Our results reveal the formation of spherical aggregates with a defined size distribution for a free monomer concentration close to the CMC. In Figure 2 are presented the schematic diagrams of the micelles for a series of surfactants with 16 hydrophobic and 18 hydrophilic units for the different surfactant architectures given in Table I. The micelles shown in these diagrams are not real conformations as obtained in standard MC, MD, or DPD simulations but instead are constructed from the most-probable configurations of the single-chain representing the surfactant in the equilibrium state. In this context, the configuration with the greatest probability is highlighted for every aggregate, which is a useful tool to help visualize the distribution of the different species composing the surfactant inside the micelles. As can be observed, the micelle cores are occupied by hydrophobic blocks and are surrounded by a non-uniform shell of hydrophilic units. The aggregation numbers N_{agg} and the CMCs predicted in this work at 25 °C under the SCMF theory are presented in Table II together with experimental available data. As expected, an increase in the aggregation number and a decrease of the CMC are found with an increase in the number of hydrophobic units for a given chain architecture. The validity of the results can be supported when comparing the CMC values predicted in this work with available experimental data for diblock (linear) and branched surfactants, where in both cases, a good quantitative agreement is obtained. The same trend has been reported in theoretical,[48] simulation,[27,38,49,50] and experimental[14,46,51,52] works. Of particular interest in this article is the behavior of the CMC with respect to the surfactant architecture keeping constant the total number of hydrophobic and hydrophilic blocks. To do so, we have chosen three series of surfactants with a constant number of units, see Figure 3, where a significant difference for the CMC depending on the surfactant geometry can be observed for all systems. For the sake of simplicity, we abbreviate the notation given in Table I for diblock (linear), branched, gemini, and triblock with central hydrophobic and hydrophilic blocks chain architectures to CE, ICE, GemE, ECE, and CEC respectively. Starting from the CE linear diblock surfactants, a

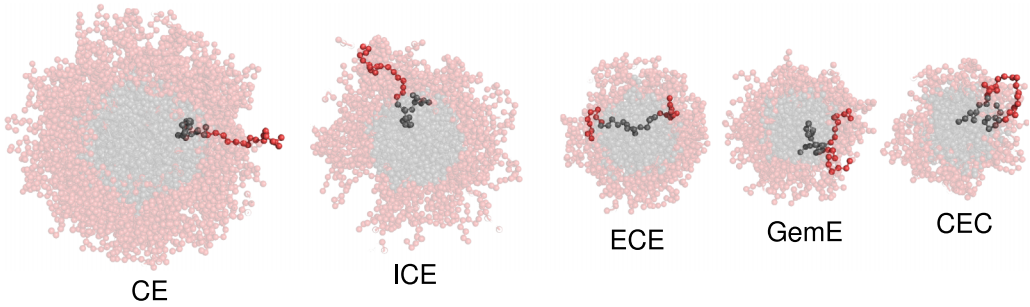

FIG. 2. Schematic cross-sections of aggregates corresponding to the minimum of the standard chemical potential for surfactants with $n = 16$ and $m = 18$ hydrophobic and hydrophilic units, respectively, for the geometries specified in Table II. The highlighted conformations refer to the surfactants with the highest probability while the others are half of the total aggregation number of the following most probable configurations.

slight increase of the CMC is observed for the branched ICE geometry which can be attributed to an increase in the steric interactions in the interior of the aggregates for the branched tail in comparison to the linear case, producing a higher free energy that causes the process to be less favorable thereby increasing the CMC. This result has also been reported in DPD simulations[49] and experimental measurements for nonionic surfactants[14] and can be explained also in terms of the enthalpic and entropic excess quantities for both cases as can be observed in Figure 4. Here, the enthalpy for the CE geometry is more negative than for the ICE case, indicating a more favorable energetic state, however, the entropy is slightly less negative for the ICE surfactant giving the opposite effect; that is, the packing of branched molecules is less adverse in comparison to the CE architecture. Despite this, the enthalpic-entropic balance favors the CE aggregation manifested in the lower CMC as stated. When considering triblock ECE and gemini GemE configurations, a general increase in the CMC of at least two times can be observed when comparing with the reference CE geometry. This is mainly due to a higher excess enthalpy produced by an increase of the interfacial core-water contact per surfactant coming from the two hydrophobic-hydrophilic contacts. On the other hand, a smaller loss of packing entropy is observed because of the hindrance of packing head groups outside the core. This can be observed when comparing analogous linear tail systems ECE and CE or branched tail GemE and ICE, but changing in both cases the number of hydrophilic blocks, as can be observed in Figure 4, this change will be consequently reflected in the changes of entropy and enthalpy excess values. Nevertheless, the enthalpic contribution is dominant in both cases with respect to the packing entropy, resulting in a less negative standard chemical potential indicating that the surfactants become more soluble thus giving a higher CMC as was reported in experiments[53] and in lattice MC simulations[25] for similar linear triblock and diblock systems.

TABLE II. Experimental and predicted CMCs from the SCMF theory together with aggregation numbers for the chain architectures under study. CMC values are given in mmol/L.

Surfactant	CMC_{SCMF}	CMC_{exp}	N_{agg}
	Diblock (linear)		
C_6E_6	117	68.5[a]	112
C_8E_6	10.4	9.80[b]	190
C_8E_8	13.6	10[b]	170
$C_{10}E_9$	1.46	1.30[a]	227
$C_{12}E_{20}$	0.518	0.1[c]	273
$C_{16}E_{18}$	0.0051	0.0003,[b] 0.002[d]	405
	Branched		
IC_6E_6	124	96.4[a]	94
IC_8E_6	12.4	21.4[a]	138
IC_8E_8	15.4	...	120
$IC_{10}E_9$	1.89	2.98[a]	143
$IC_{12}E_{20}$	0.551	...	156
$IC_{16}E_{18}$	0.0080	...	193
	Gemini		
Gem_8E_8	42	...	56
$Gem_{12}E_{20}$	2.37	...	54
$Gem_{16}E_{18}$	0.0207	...	96
	Triblock		
$E_4C_8E_4$	39	...	64
$E_{10}C_{12}E_{10}$	2.13	...	65
$EC_{16}E_9$	0.0210	...	120
$C_8E_{18}C_8$	0.151	...	89

[a]From Ref. 46 at 25 °C.
[b]From Ref. 47 at 25 °C.
[c]Value from Ref. 47 for surfactant $C_{12}E_{25}$.
[d]Value from Ref. 46 for surfactant $C_{16}E_{12}$.

A similar situation can be observed in the case of the triblock copolymers with two hydrophobic ends, CEC, where a high CMC is predicted in comparison with the other geometries. In this case, a less negative entropic penalty is found together with a less negative enthalpic compensation. In the case of the enthalpy, the two hydrophobic extremes of a surfactant must enter into the core of the micelle thus increasing the steric interactions and consequently the excess enthalpy similar to the GemE situation. For aggregates to form, the surfactants must form a loop, which is not the case of any of the other systems. Effectively, this situation will produce a packing entropy contribution. According to our calculations, for the ECE case, a surfactant in an equilibrium aggregate possesses a packing entropy $\langle S_N \rangle / N = -19.19\ k$ and enthalpy $\langle U_N \rangle / N = 29.69\ kT$ in contrast to the values of $-17.04\ k$ and $34.26\ kT$ for the CEC surfactants, which means that packing surfactants in CEC aggregates have a gain in entropy but a high energetic

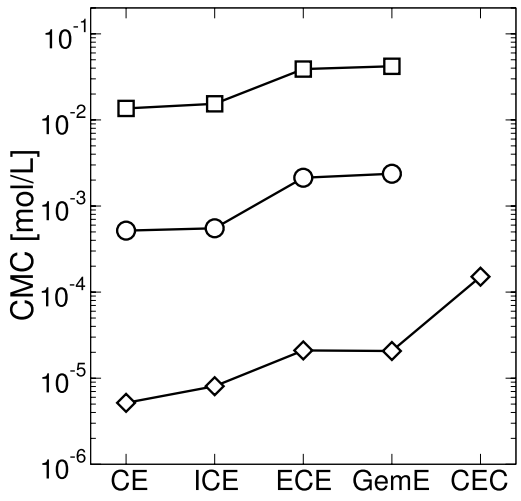

FIG. 3. Predicted CMC depending on the block architecture for three surfactants with defined numbers of hydrophobic, C_n, and hydrophilic, E_m, units. Empty squares refer to surfactants with $\{n,m\}=\{8,8\}$, empty circles represent the set $\{n,m\}=\{12,20\}$, and empty diamonds depict $\{n,m\}=\{16,18\}$. The solid line is included to help guide the eye.

cost when comparing to the ECE system. In both cases, similar excess contributions were found for the free surfactants in the bulk solution ($\langle S_1\rangle \approx 1.1\ k$ and $\langle U_1\rangle \approx 65\ kT$). Our results for the excess quantities are qualitatively similar to those found in previous lattice MC simulations[26] for triblock HTH and THT copolymers, as well as experimental CMCs[10,53] together with simulation predictions.[25,27,49]

Given that for the same number of monomers, similar CMCs are obtained in the case of CE and ICE or ECE and GemE, we turn our attention to another equilibrium property, namely, the equilibrium aggregation numbers N_{agg} which are presented in Figure 5. As can be observed, a systematic variation of the aggregation numbers depending on the block architecture is found. This situation is in contrast to the CMC where different architectures can exhibit a similar value. Keeping constant the hydrophilic block and varying the hydrophobic configurations, as in the case of CE and ICE, produces a decrease of the aggregation number for the branched case. This can be explained in terms of a compacting of the core for the ICE species in comparison with the linear one, resulting in a reduction of the free energy for a lower aggregation number, which is similar to some reported simulation results.[15,49] In the case of surfactants with two hydrophilic segments such as ECE and GemE, an increase of the interfacial area per surfactant between the core and the solvent is produced, leading to a decrease in the steric repulsion between hydrophilic units in the shell of the aggregate, thus requiring a lower number of surfactants to minimize the free energy in contrast to the diblock (linear) case. In addition to this, we have found a higher aggregation number for ECE surfactants compared to GemE. Despite a similar arrangement of the surfactants in the aggregated state, a slightly higher packing entropy penalty is imposed for the geminis due to the restriction in the accommodation of tails in the core because of the branching in the hydrophobic segments; contrarily, the triblock case can accommodate the tails more readily. This small entropic difference affects quantitatively the aggregation number in a similar manner for diblock (linear) surfactants with different head groups.[43] On the other hand, we have found a smaller value of the aggregation number for CEC when comparing with ECE case which is contrary to previous results given by grand-canonical MC techniques.[25–27] In particular, Kim and Jo[26] determined the excess entropy and enthalpy for symmetric triblock systems HTH and THT with fixed length. The excess quantities of the THT surfactants are found to be less negative in comparison to the HTH case,[26,27] which is qualitatively similar to the results presented in Figure 4. The behavior of the packing entropy is related to the value of the equilibrium aggregation number, N_{agg}, as has been stated before for linear triblock[26,27] and diblock[43] systems. For this reason, we believe that the qualitative discrepancy between our predictions for the aggregation numbers and the ones reported by Kim and Jo[26,27] and Panagiotopoulos *et al.*[25] is possibly due to the absence of dangling and bridge conformations in our SCMF calculations for the CEC surfactant which has been demonstrated to be relevant for the packing entropy and therefore the aggregation numbers. Despite the fact that we are limited by the one-dimensional geometry effectively at infinite dilution imposed in our simulations leading to neglect the possibility of dangling and bridge conformations that enables the

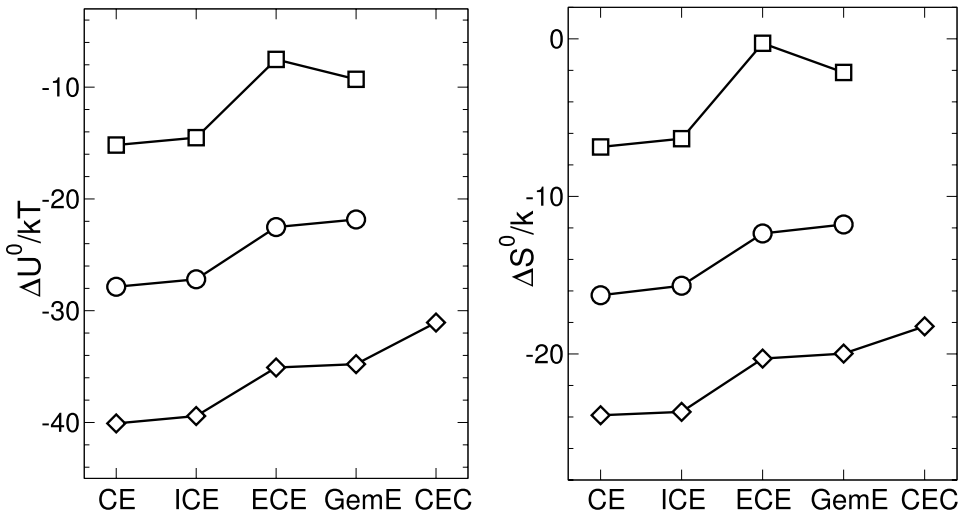

FIG. 4. Excess enthalpy and entropy per surfactant as a function of the surfactant architecture. Symbols and lines are as in Figure 3.

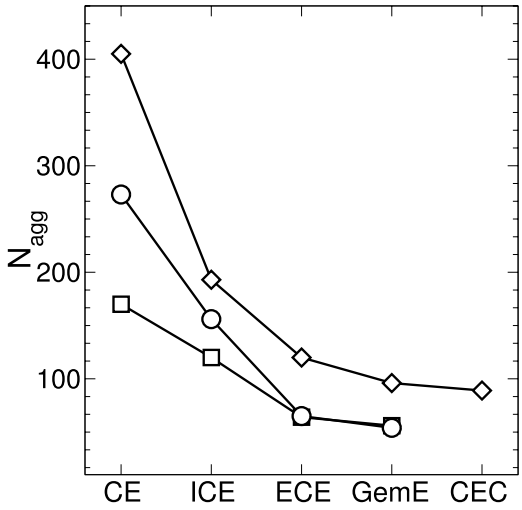

FIG. 5. Aggregation numbers for surfactants with different architectures. Symbols and lines are as in Figure 3.

possibility of connected aggregates, we expect that this will not substantially affect the calculation of the excess enthalpy but may result in an incomplete estimation of the packing entropy affecting directly the aggregation number. Although a two or even three-dimensional geometry can be implemented in the SCMF scheme to evaluate the impact of these kind of conformations, it is beyond the scope of the present work. On the other hand, these excess quantities depend on a fine balance between several contributions and so this difference with previous studies may be due instead merely to the model used or to inaccuracies from the mean-field approximation.

IV. SUMMARY

In this work, we have studied the equilibrium CMC and aggregation number for a series of poly(ethylene oxide) alkyl ethers surfactants with different block architectures but constant number of hydrophobic and hydrophilic groups. Our results reveal that, in general, triblock or branched conformations increase the solubility of the surfactants while the aggregation numbers exhibit a decreasing behavior. The behavior of the corresponding CMCs is evaluated from the excess enthalpic-entropic balance where an increase in both quantities is observed for different copolymer architectures taking as reference the diblock (linear) architectures. The results reported in this work highlight the ability of the SCMF theory to quantify the impact of the surfactant geometry on the relevant macroscopic quantities. This was carried out by means of an analysis of the thermodynamic excess variables involved in the aggregation process.

ACKNOWLEDGMENTS

F.A.G.D. acknowledges the financial support from URV through his Ph.D. scholarship.

[1]K. Kataoka, A. Harada, and Y. Nagasaki, Adv. Drug Delivery Rev. **64**, 37 (2012).
[2]C. Thompson, L. Tetley, and W. Cheng, Int. J. Pharm. **383**, 216 (2010).
[3]L. Qiu and Y. Bae, Pharm. Res. **23**, 1 (2006).
[4]Z. Wang, C. Chen, Q. Zhang, M. Gao, J. Zhang, D. Kong, and Y. Zhao, "Tuning the architecture of polymeric conjugate to mediate intracellular delivery of pleiotropic curcumin," Eur. J. Pharm. Biopharm. (published online).
[5]Y. Wang and S. M. Grayson, Adv. Drug Delivery Rev. **64**, 852 (2012).
[6]J. Liu, H. Duong, M. R. Whittaker, T. P. Davis, and C. Boyer, Macromol. Rapid Commun. **33**, 760 (2012).
[7]H. Nakamura, E. Koziolová, T. Etrych, P. Chytil, J. Fang, K. Ulbrich, and H. Maeda, "Comparison between linear and star-like HPMA conjugated pirarubicin (THP) in pharmacokinetics and antitumor activity in tumor bearing mice," Eur. J. Pharm. Biopharm. (published online).
[8]L. Lee, J. Salimon, M. A. Yarmo, R. Syafri, and M. Hisam, J. Dispersion Sci. Technol. **34**, 914 (2013).
[9]H. Altinok, G. Yu, S. K. Nixon, P. A. Gorry, D. Attwood, and C. Booth, Langmuir **13**, 5837 (1997).
[10]C. Booth, D. Attwood, and C. Price, Phys. Chem. Chem. Phys. **8**, 3612 (2006).
[11]X. Wang, J. Wang, Y. Wang, J. Ye, H. Yan, and R. K. Thomas, J. Phys. Chem. B **107**, 11428 (2003).
[12]A. A. Steinschulte, B. Schulte, S. Rutten, T. Eckert, J. Okuda, M. Moller, S. Schneider, O. V. Borisov, and F. A. Plamper, Phys. Chem. Chem. Phys. **16**, 4917 (2014).
[13]G. Bai, J. Wang, Y. Wang, H. Yan, and R. K. Thomas, J. Phys. Chem. B **106**, 6614 (2002).
[14]K. Kratzat and H. Finkelmann, Langmuir **12**, 1765 (1996).
[15]C. Lin, Y. Chen, Y. Sheng, and H. Tsao, React. Funct. Polym. **69**, 539 (2009).
[16]M. Zamurovic, S. Christodoulou, A. Vazaios, E. Iatrou, M. Pitsikalis, and N. Hadjichristidis, Macromolecules **40**, 5835 (2007).
[17]D. Liu and C. Zhong, Polymer **49**, 1407 (2008).
[18]M. La Rosa, A. Uhlherr, C. H. Schiesser, K. Moody, R. Bohun, and C. J. Drummond, Langmuir **20**, 1375 (2004).
[19]T. Taddese, P. Carbone, and D. L. Cheung, Soft Matter **11**, 81 (2015).
[20]A. G. Goicochea, M. Romero-Bastida, and R. López-Rendón, Mol. Phys. **105**, 2375 (2007).
[21]Z. Wang, Y. Li, Y. Guo, and H. Zhang, J. Dispersion Sci. Technol. **34**, 1020 (2013).
[22]G. Illya, R. Lipowsky, and J. C. Shillcock, J. Chem. Phys. **122**, 244901 (2005).
[23]V. Firetto, M. A. Floriano, and A. Z. Panagiotopoulos, Langmuir **22**, 6514 (2006).
[24]K. E. Hart, L. J. Abbott, M. Lísal, and C. M. Colina, J. Chem. Phys. **141**, 204902 (2014).
[25]A. Z. Panagiotopoulos, M. A. Floriano, and S. K. Kumar, Langmuir **18**, 2940 (2002).
[26]S. H. Kim and W. H. Jo, Macromolecules **34**, 7210 (2001).
[27]S. H. Kim and W. H. Jo, J. Chem. Phys. **117**, 8565 (2002).
[28]L. Rekvig, M. Kranenburg, J. Vreede, B. Hafskjold, and B. Smit, Langmuir **19**, 8195 (2003).
[29]D. R. Jackson, A. Mohareb, J. MacNeil, M. S. G. Razul, D. G. Marangoni, and P. H. Poole, J. Chem. Phys. **134**, 204503 (2011).
[30]J. Zhou and A. Shi, Macromol. Theory Simul. **20**, 690 (2011).
[31]P. N. Hurter, J. M. H. M. Scheutjens, and T. A. Hatton, Macromolecules **26**, 5592 (1993).
[32]P. Linse, J. Phys. Chem. **97**, 13896 (1993).
[33]A. De Nicola, T. Kawakatsu, and G. Milano, Macromol. Chem. Phys. **214**, 1940 (2013).
[34]V. G. de Bruijn, L. J. P. van den Broeke, F. A. M. Leermakers, and J. T. F. Keurentjes, Langmuir **18**, 10467 (2002).
[35]Y. Lauw, F. A. M. Leermakers, and M. A. Cohen Stuart, J. Phys. Chem. B **110**, 465 (2006).
[36]M. Monzen, T. Kawakatsu, M. Doi, and R. Hasegawa, Comput. Theor. Polym. Sci. **10**, 275 (2000).
[37]A. Ben-Shaul, I. Szleifer, and W. M. Gelbart, J. Chem. Phys. **83**, 3597 (1985).
[38]A. Gezae Daful, V. A. Baulin, J. Bonet Avalos, and A. D. Mackie, J. Phys. Chem. B **115**, 3434 (2011).
[39]J. Bonet Avalos, A. D. Mackie, and S. Díez-Orrite, Macromolecules **37**, 1143 (2004).
[40]J. N. Israelachvili, *Intermolecular and Surface Forces* (Elsevier, San Diego, CA, 2011).
[41]Z. A. Al-Anber, J. Bonet Avalos, and A. D. Mackie, J. Chem. Phys. **122**, 104910 (2005).
[42]M. N. Rosenbluth and A. W. Rosenbluth, J. Chem. Phys. **23**, 356 (1955).
[43]C. M. Care and T. Dalby, EPL **45**, 38 (1999).
[44]Z. A. Al-Anber, J. Bonet i Avalos, M. A. Floriano, and A. D. Mackie, J. Chem. Phys. **118**, 3816 (2003).

[45]A. G. Daful, J. B. Avalos, and A. D. Mackie, Langmuir **28**, 3730 (2012).
[46]M. Mattei, G. M. Kontogeorgis, and R. Gani, Ind. Eng. Chem. Res. **52**, 12236 (2013).
[47]A. Berthod, S. Tomer, and J. G. Dorsey, Talanta **55**, 69 (2001).
[48]R. Nagarajan, Chem. Eng. Commun. **55**, 251 (1987).
[49]Y. Lin, M. Wu, Y. Sheng, and H. Tsao, J. Chem. Phys. **136**, 104905 (2012).
[50]F. A. García Daza and A. D. Mackie, J. Phys. Chem. Lett. **5**, 2027 (2014).
[51]T. Kuwamura and H. Takahashi, Bull. Chem. Soc. Jpn. **45**, 617 (1972).
[52]W. L. Hinze and E. Pramauro, Crit. Rev. Anal. Chem. **24**, 133 (1993).
[53]C. Booth and D. Attwood, Macromol. Rapid Commun. **21**, 501 (2000).